

Nonmuscle myosins II-B and Va are components of detergent-resistant membrane skeletons derived from mouse forebrain

Jane E. Ishmael^{1,3}, Masa Safic¹, David Amparan¹, Walter K. Vogel¹, Tuyen Pham¹, Kevin Marley², Theresa M. Filtz¹ and Claudia S. Maier^{2,3}

Department of Pharmaceutical Sciences, College of Pharmacy¹, Department of Chemistry², and the Environmental Health Sciences Center³, Oregon State University, Corvallis, Oregon 97331.

To whom correspondence should be addressed:

Jane E. Ishmael, Ph.D.
Department of Pharmaceutical Sciences
College of Pharmacy
Oregon State University
Corvallis, Oregon 97331
Tel: (541) 737-5783
Fax: (541) 737-3999
Email: jane.ishmael@oregonstate.edu

and

Claudia S. Maier, Ph.D.
Department of Chemistry
Oregon State University
Corvallis, Oregon 97331
Tel: (541) 737-9533
Fax: (541) 737-2062
Email: claudia.maier@oregonstate.edu

Abstract

Myosins are actin-based molecular motors that may have specialized trafficking and contractile functions in cytoskeletal compartments that lack microtubules. The postsynaptic excitatory synapse is one such specialization, yet little is known about the spatial organization of myosin motor proteins in the mature brain. We used a proteomics approach to determine if class II and class V myosin isoforms are associated with Triton X-100-resistant membranes isolated from mouse forebrain. Two nonmuscle myosin isoforms (II-B and Va), were identified as components of lipid raft fractions that also contained typical membrane skeletal proteins such as non-erythrocyte spectrins, actin, alpha-actinin-2 and tubulin subunits. Other raft-associated proteins included lipid raft markers, proteins involved in cell adhesion and membrane dynamics, receptors and channels including glutamate receptor subunits, scaffolding and regulatory proteins. Myosin II-B and Va were also present in standard postsynaptic density (PSD) fractions, however retention of myosin II-B was strongly influenced by ATP status. If homogenates were supplemented with ATP, myosin II-B could be extracted from PSD I whereas myosin Va and other postsynaptic proteins were resistant to extraction. In summary, both myosin isoforms are components of a raft-associated membrane skeleton and are likely detected in standard PSD fractions as a result of their intrinsic ability to form actomyosin. Myosin IIB, however, is loosely or more peripherally associated with the PSD than myosin Va, which appears to be a core PSD protein.

Keywords lipid raft, mass spectrometry, actin cytoskeleton, proteomics, postsynaptic density, myosin II, myosin V

Multiple members of the myosin superfamily of motor proteins are present in neurons (Bridgman 2004), and isoforms representing classes I, II, V, VI and XVIII have specifically been identified at synapses activated by the excitatory neurotransmitter glutamate (Cheng et al. 2006; Collins et al. 2006). Myosins are protein complexes comprised of heavy chains and varying numbers of resident light chains (Sellers 2000). The myosin heavy chain head region binds directly to actin filaments (F-actin) in a cyclical manner to form the complex known as actomyosin, and is rapidly dissociated from actin in the presence of ATP (Geeves et al. 2005). Myosins can therefore be clearly distinguished from kinesins and dyneins, which are microtubule-based motors (Woehlke and Schliwa 2000), and may have critical functions in regions of the neuronal cytoskeleton that lack microtubules (Bridgman 2004). Dendritic spines are examples of such cytoskeletal specializations in that they are enriched in actin, yet are devoid of microtubules (Harris and Kater 1994). Spines protrude away from the dendritic shaft to form the postsynaptic side of an excitatory synapse and account for over 90% of all excitatory synapses in the CNS (Harris and Kater 1994). These unique structures can also be further characterized by the presence of a distinct organelle that lies directly below the postsynaptic membrane at the head of the spine known as the postsynaptic density (PSD) (Kennedy 1998). The PSD is functionally organized for optimum signal transduction, and contains an array of scaffolding and cytoskeletal proteins that hold receptors, enzymes and other signaling proteins in close proximity to one another (Sheng and Sala 2001). The physical continuum that is achieved between the plasma membrane and PSD is highlighted by the fact that membrane-bound glutamate receptors, which mediate the majority of excitatory neurotransmission in the CNS, bind directly to proteins located within the PSD via their intracellular carboxyl tail domains (Kornau et al. 1995).

Advances in mass spectrometry and bioinformatics have continued to reveal the complexity of the postsynaptic excitatory synapse through the use of several complementary approaches (Cheng et al. 2006; Collins et al. 2006). For

example, the first group to use mass spectrometry to identify proteins associated with the N-methyl-D-aspartate (NMDA) subtype of glutamate receptor isolated complexes by immunoprecipitation or retention on an immunoaffinity column (Husi et al. 2000). In a parallel approach, another group isolated the major components of the PSD from detergent resistant PSD fractions (Walikonis et al. 2000). Although many proteins identified in these initial studies were common to both data sets, the myosin heavy chains identified by each group represented two distinct classes of myosin motor (Sheng and Lee 2000). Peptides corresponding to the heavy chain of nonmuscle myosin II-B were coimmunoprecipitated in a complex of proteins associated with the NMDA receptor (Husi et al. 2000), whereas peptides corresponding to myosin Va heavy chain were identified in PSD-fractions (Walikonis et al. 2000). We have recently determined that a light chain of myosin II, interacts directly with NMDAR1 (NR1) and NMDAR2 (NR2) subunits of the NMDA receptor (Amparan et al. 2005), providing additional evidence for a close association of the NMDA receptor with a myosin II motor (Husi et al. 2000). The physiological properties (Lei et al. 2001; Ryu et al. 2006) and morphology (Ryu et al. 2006) of glutamatergic synapses are also sensitive to pharmacological manipulation of the myosin II complex. Taken together, these findings raised the possibility that myosin II may be more closely associated with a membrane-bound glutamate receptor complex rather than the postsynaptic density.

The study of other cell types, particularly those of the hematopoietic system, has revealed an actin-rich submembrane cytoskeleton that is intimately associated with lipid rafts (Rodgers and Zavzavadjian 2001; Nebl et al. 2002; Valensin et al. 2002). Lipid rafts are ordered cholesterol and sphingolipid-rich domains within the plasma membrane that serve as platforms for lateral organization of cell signaling and membrane traffic (Harder and Simons 1997). In contrast to proteins of the PSD which are resistant to detergent-extraction due to strong association with the cytoskeleton (Cho et al. 1992; Kennedy 1998), proteins that associate with raft membranes are resistant to detergent-extraction by virtue of

their proximity to membrane lipids (Harder and Simons 1997). Glutamate receptor subunits and associated scaffolding proteins have previously been detected in lipid raft fractions isolated from rat brain (Hering et al. 2003). Moreover, lipid rafts are abundant in neuronal dendrites where they appear to influence the shape and density of dendritic spines (Hering et al. 2003). In the present study, we took advantage of the known association of cytoskeletal proteins with raft membranes to determine which myosin isoforms may be components of the submembrane cytoskeleton rather than the core PSD. We used mass spectrometry to identify major proteins that associate with lipid rafts isolated from detergent-resistant forebrain membranes by buoyant-density centrifugation. We report that myosin II-B and myosin Va are both associated with lipid raft fractions and are likely components of the submembrane cytoskeleton. Both myosin isoforms were also retained in detergent-resistant PSD fractions, however detection of myosin II-B is strongly influenced by the presence of ATP. Myosin II-B can be dissociated from the cytoskeleton if the ATP status of the tissue homogenate is enhanced, whereas myosin Va and other postsynaptic proteins remain core components of Triton X-100-extracted PSD fractions.

Materials and methods

Antibodies

Primary antibodies used for immunoblot analyses included: isoform specific antibodies to myosin II heavy chains A and B (both from Covance, Princeton, NJ), anti-myosin Va (LF-18; Sigma-Aldrich, Saint Louis, MO), anti-PSD-95 (Affinity Bioreagents Inc., Golden, CO), anti-actin (A5060; Sigma-Aldrich, Saint Louis, MO), anti-alpha actinin-2 (clone BM 75.2; Sigma-Aldrich, Saint Louis, MO), anti-caveolin (Santa Cruz Biotechnology, Santa Cruz, CA), anti-transferrin receptor (Invitogen, Carlsbad, CA), anti-NMDAR1 (clone 54.1 PharMingen, San Diego, CA), anti-NMDAR2B (Chemicon, Temecula, CA) and anti-GluR2/3 (Chemicon, Temecula, CA).

Preparation of detergent-resistant membrane fractions

Frozen adult mouse forebrain (Pel-Freez Biologicals, Rogers, AR) was thawed on ice, weighed and homogenized in a buffer containing 320 mM sucrose, 25 mM HEPES, 2 mM sodium orthovanadate, 1 mM sodium fluoride pH 7.4, plus protease inhibitors (1 μ g/mL pepstatin, 10 μ g/mL apoprotinin, 5 μ g/mL leupeptin and 100 μ g/mL 4-[2-aminoethyl]benzenesulfonyl fluoride/Pefabloc) and centrifuged at 800 x g, for 10 minutes at 4°C to pellet nuclei (P1). The resulting supernatant was carefully removed and subjected to centrifugation at 9,200 x g for 15 min. The resulting pellet (P2) was then resuspended in a buffer containing 1% Triton X-100 in 25 mM Hepes, 1mM EDTA plus protease inhibitors (pH 7.4) with rotation for 1 hour at 4 °C. The brain extract was transferred to a centrifuge tube, mixed with an equal volume of 90% sucrose, and overlaid with 35%, 25%, 15% and 5% sucrose each containing 1% Triton X-100 plus protease inhibitors. Detergent-resistant membranes were routinely prepared from two mouse forebrains. Each sample was divided and fractionated on two independent sucrose gradients. After centrifugation at 230,000 x g for 24 hours at 4 °C, eleven 1 ml fractions were collected from the top of the tube and stored at 4 °C whilst equal volumes of each fraction were analyzed for cholesterol (Amplex red cholesterol assay kit; Molecular Probes) and protein content using a detergent

compatible bicinchoninic acid (BCA) assay (Pierce Biotechnology Inc., Rockford, IL). Equal volumes of each fraction were also routinely tested for the presence of caveolin and transferrin receptor by immunoblot analysis.

Preparation of samples for mass spectrometry

Lipid raft and control fractions were separated by one-dimensional polyacrylamide gel electrophoresis (PAGE) on a 4-12% pre-cast Criterion gel (BioRad Laboratories, Hercules, CA). After electrophoresis, gels were washed three times for 5 min in deionized (DI) water. Proteins were visualized by Coomassie blue stain (Bio-Safe, BioRad), rinsed and stored overnight in DI water at room temperature. Bands were excised from the gel, rinsed twice for 15 min. in DI water and twice for 15 min in a solution containing 50% acetonitrile and 50% ammonium bicarbonate (50 mM) to remove the Coomassie blue stain from the gel pieces. Gel plugs were washed and dehydrated in 100% acetonitrile for approximately 20 min until opaque, the acetonitrile decanted and the sample dried in a vacuum centrifuge at room temperature. Trypsin (Trypsin Gold V528, Promega, Madison, WI) was prepared as a 0.5 $\mu\text{g}/\mu\text{l}$ stock solution in 1% acetic acid, and diluted 40-fold in ammonium bicarbonate (25 mM) to a working trypsin solution of 12.5 $\text{ng}/\mu\text{l}$ (pH \approx 8.0). Samples were rehydrated in fresh trypsin solution (12.5 $\text{ng}/\mu\text{l}$) for 45 min on ice, to allow the trypsin to diffuse into the gel plug. Excess trypsin solution was removed, ammonium bicarbonate (25 mM) added and samples allowed to digest overnight at 37°C. The digestion solution was recovered the next morning, and gel plugs subjected to two additional extractions for 15 min each in 50% acetonitrile/50% ammonium bicarbonate (50 mM) to recover additional peptides. Gel pieces were subjected to a final extraction in 100% acetonitrile, the extracts pooled and concentrated to dryness in a vacuum centrifuge at room temperature.

Mass spectrometry

Liquid chromatograph (LC) tandem mass spectrometry (MS/MS) was performed using a quadrupole orthogonal time-of-flight mass spectrometer (Q-ToF Ultima

Global, Micromass/Waters, Manchester, UK) equipped with an Electrospray ionization (ESI) source and coupled to a nanoAcquity Ultra Performance LC (Waters, Milford, MA). Peptide mixtures were trapped and washed on a nanoAcquity column (Symmetry C₁₈, 5 μ m, 180 μ m x 20 mm) for 3 min using 2 % acetonitrile containing 0.1 % formic acid at 4 μ L/min. Peptide fractionation was accomplished using an in-house packed 12 cm x 75 μ m Jupiter C₅ or C₁₈ (5 μ m; Phenomenex Inc., Torrance, CA) picofrit column (New Objectives, Woburn, MA). Peptides were eluted using a binary gradient system consisting of solvent A, 0.1 % formic acid and solvent B, acetonitrile containing 0.1 % formic acid.

The electrospray ion source was operated in the positive ion mode with a spray voltage of 3.5 kV. The data-dependent MS/MS mode was used with a 0.6 s survey scan and 2.4 s MS/MS scans on the three most abundant ion signals in the MS survey scan, with previously selected m/z values being excluded for 60 s. The collision energy for MS/MS (25 to 65 eV) was dynamically selected based on the charge state of the ion selected by the quadrupole analyzer (q1). Mass spectra were calibrated using fragment ions of Glu¹-fibrinopeptide B (MH⁺ 1570.6774 Da, monoisotopic mass). In addition, to compensate for temperature drifts, lock mass correction was used every 30 s for 1 scan using the doubly charged ion of Glu¹-fibrinopeptide B ([M+2H]²⁺ 785.8426 Da, monoisotopic mass).

MS/MS Data Analysis

Mascot software (Matrix Science, London, UK) was used to aid in the interpretation of tandem mass spectral data. Searches were performed using the SwissProt (taxonomy *mus musculus*) database. Trypsin/P was selected as the digesting enzyme allowing for the possibility of up to three missed cleavage sites. The following variable peptide modifications were allowed: carbamidomethyl (C), deamidation (NQ), phosphorylation (STY), pyro-Glu (N-terminal E) and pyro-Glu (N-term Q). In addition, possible oxidation of methionine (M) and neutral loss of

CH₃SOH (monoisotopic mass 63.9983) was considered. Mass tolerances were set to ± 0.2 Da for the precursor ion and ± 0.2 Da for the fragment ions.

Peak list files (pkl files) were created using Masslynx software (Waters, Milford, MA, USA) using a function that smoothes and calculates centroids of the data. Mascot calculates the so-called Mowse core as statistical parameter to validate the peptide identification. This score is based on the probability (p) that a peptide identified from the experimental fragment matches a peptide in a protein database, and is calculated as: Mowse score = $-10 \times \log(p)$. A random match will have a high probability value and low Mowse score, while a valid match will have a low probability value and a high Mowse score. Tandem mass spectra that obtained a peptide score >30 were considered as positive hits. Mascot ranks the quality of the peptide matches and sums the scores of acceptable peptides to calculate a total protein score. A protein identification was considered as 'high confidence' identification if at least two peptides with score >30 were available (Table 1). Protein identifications were considered 'tentative' or 'low confidence' identifications when only one peptide identification was available, even when the respective tandem mass spectrum had a score better than 30 (Supplementary Table 1). Selected tandem mass spectral data were evaluated manually and annotated using the nomenclature of (Biemann 1988).

Preparation of synaptosomes and postsynaptic density (PSD) fractions.

Adult male Sprague-Dawley rats (Simonsen Laboratories Inc., Gilroy, CA) weighing 350-400 g were euthanized by CO₂ narcosis in accordance with protocols approved by the Institutional Animal Care and Use Committee at Oregon State University, Corvallis, OR. Brains were rapidly removed and the forebrain dissected as previously described (Carlin et al. 1980). Synaptosomes were prepared by discontinuous sucrose density-gradient according to the method of Carlin and coworkers (Carlin et al. 1980). Postsynaptic density fractions (I, II and III) were prepared from synaptosome fractions according to the method established by Cho and coworkers (Cho et al. 1992), resulting in: PSD I

(15 min incubation with 0.5% Triton X-100), PSD II (PSD I plus a second 15 min incubation with 0.5% Triton X-100) and PSD III (PSD I plus a second 10 min incubation with 3% Sarcosyl). For some studies, the synaptosome fraction was divided and incubated for 15 min with ice-cold 0.5% Triton X-100 in the presence or absence of 10 mM ATP prior to centrifugation at 32,000 x g for 20 min. at 4°C to obtain PSD I + ATP and PSD I, respectively. All protein concentrations were determined using the method of Lowry et al. (Lowry et al. 1951).

Immunoblot Analysis

Equal volumes of each fraction were separated by sodium dodecyl sulfate (SDS)-PAGE and electrotransferred to a nitrocellulose membrane (Amersham Biosciences Inc., Piscataway, NJ). Nitrocellulose membranes were incubated with 5% (w/v) milk powder in Tris-buffered saline (TBS) containing 0.05% Tween-20 (TBST) for 1 hr. at room temperature. Membranes were incubated with appropriate primary antibodies diluted in TBS with milk powder with gentle rotation either overnight at 4°C, or for 2 hr at room temp. At the end of the primary antibody incubation, membranes were washed in TBST (3 x 10 min at room temperature) and TBS (1 x 10 min at room temperature), before incubation for 90 min at room temperature with appropriate horseradish peroxidase-conjugated secondary antibodies (Calbiochem). Membranes were finally washed with TBST and TBS as described above, and immune complexes revealed using a chemiluminescence assay (Roche, Indianapolis, IN).

Results.

Characterization of a detergent-resistant lipid raft fraction.

We isolated a lipid raft fraction from adult forebrain to determine if class II and class V myosins are differentially associated with membranes. Towards this goal, a crude membrane fraction was extracted in 1% Triton X-100 for 60 minutes at 4°C. The detergent-resistant lipid raft fraction was then isolated by flotation in a 5% to 35%, buoyant-density linear sucrose gradient in the presence of detergent. Eleven 1 mL fractions (Fig. 1A) were subsequently collected after centrifugation for 24 hours, and each fraction assayed for cholesterol and protein content (Fig. 1B). Under these conditions a low-density fraction characterized by high cholesterol (Fig 1B, dark squares), and relatively low total protein (Fig 1B, open circles) was consistently found in the fourth sample (fraction 4). Immunoblot analysis of samples taken from each fraction also revealed the presence of the raft marker protein caveolin in fraction 4 (Fig. 1C). We chose caveolin as a positive control (or raft marker) as previous studies have demonstrated that “caveolin-type” rafts from rat brain likely contain NMDA receptors and PSD-95 (Hering et al. 2003). The non-raft associated protein transferrin receptor was detected only in high-density fractions towards the bottom of the gradient (Fig. 1C). Fraction 4 was therefore designated the lipid raft fraction for further study on the basis of several criteria: low buoyant density, high cholesterol, the presence of caveolin, the exclusion of transferrin receptor and low protein content relative to high density fractions at the bottom of the gradient. Forebrain was chosen for this analysis, and subsequent analyses of postsynaptic density fractions, as excitatory synapses have been intensively studied in this area, which is easily dissected for biochemical studies and includes cortex, striatum and hippocampus (Carlin et al. 1980; Husi et al. 2000).

Identification of major raft-associated proteins by mass spectrometry

Raft-associated proteins in fraction 4 were separated by one-dimensional gel electrophoresis and visualized with Coomassie blue stain (Fig. 2). The pattern observed after Coomassie blue staining of fraction 4 was highly reproducible;

figure 4 shows three independent lipid raft fractions each from a separate buoyant-density gradient (fraction 4a, 4b and 4c). The stained gel was photographed and eight major bands visible with the naked eye, as well as the region predicted to contain heavy chains corresponding to class II or V myosin isoforms, were identified and excised for in-gel digestion with trypsin (Fig. 2, lane 5).

Forty-four proteins were identified with high confidence from nine gel regions that were submitted for tandem mass spectrometry (Table 1). A high confidence match was assigned on the basis that at least two tandem mass spectra yielded peptide scores better than 30. A further seventeen proteins were designated as tentatively identified (i.e. identified with low confidence) on the basis of single peptide identifications. It should be noted, however, that the corresponding tandem mass spectral data were partly of very high quality (peptide score > 75) and the lowest scoring tandem mass spectrum that was used for identification assignment yielded a score of 37 (see Supplementary Table 1).

Cytoskeletal proteins such as spectrin, actin-, microtubule- and neurofilament-based proteins were well represented in the major bands excised from fraction 4, accounting for 30% of all proteins identified by mass spectrometry (Table 1 and Supplementary Table 1). The positive identification of alpha and beta forms of spectrin and actin was particularly significant as these proteins are also prototypical components of membrane skeletons derived from other cell types that are not complicated the presence of a PSD (De Matteis and Morrow 2000; Nebl et al. 2002; Ciana et al. 2005). Most interestingly, the myosin heavy chains corresponding to nonmuscle myosin II-B (Accession number Q61879; also known as myosin-10), and nonmuscle myosin Va (Accession number Q99104), were identified as raft-associated proteins in gel region 2 (see below, Figures 3 and 4, Tables 1 and 2). Approximately 30 % of all proteins identified by mass spectrometry could be classified as proteins involved in cell adhesion and various aspects of membranes dynamics (Table 1 and Supplementary Data). Receptors, channels, regulatory proteins such as heteromeric G-proteins, and enzymes represented a further 24% of all proteins identified by mass spectrometry.

Several scaffolding proteins were also identified as raft-associated proteins. These included Homer 1, a regulatory metabotropic glutamate receptor-interacting protein that is enriched at excitatory synapses (Xiao et al. 1998), septin-5 and RAB6-interacting protein (Table 1 and Supplementary Table 1). Mitochondrial proteins and proteins involved in metabolism also accounted for a small percentage of raft-associated proteins (Table 1 and Supplementary Data). As anticipated, at least 20% of all proteins identified across categories contained motifs associated with posttranslational modifications to target proteins to lipid domains. Lipid modifications included: (1) glychosphatidylinositol (GPI)-anchored proteins such as Thy-1, contactins, neurotrimin, opioid-binding protein, neuronal growth regulator 1 and limbic-associated membrane protein (Table 1 and Supplementary Table 1), (2) palmitoyl moieties in proteins such as neuromodulin and paralemmin, and (3) myristoylation modifications in proteins such as myristoylated alanine-rich C-kinase substrate (MARKCS), Src and brain acid soluble protein 1 (Table 1). The identification of the GPI-anchored protein Thy-1 was significant, as this protein is considered a common biomarker of lipid rafts (Pike 2004). It is important to note however, that Thy-1 may not necessarily be located in the same type of lipid raft as caveolin (Hering et al. 2003), the cholesterol binding protein used as a raft marker in our original characterization of the lipid raft fraction (Fig. 1). In keeping with the idea that rafts are not homogeneous entities *in vivo* (Pike 2004), it is more likely that a heterogeneous population of lipid rafts and associated proteins was isolated under the conditions of the present study. Nevertheless, the overall profile of raft-associated proteins identified by mass spectrometry was consistent with Triton-X-100-resistant membrane fractions isolated from other cell types (Nebl et al. 2002; Bae et al. 2004; Li et al. 2004; Ciana et al. 2005). This subset of proteins, representing major components of the raft-associated proteome, serves to validate our approach and indicates that Triton-X-100-resistant membranes derived from forebrain are likely connected to a submembrane cytoskeleton that also contains actin-based myosin motors.

Tandem mass spectrometric identification of the nonmuscle myosins II-B and Va.

Each class of the myosin superfamily contains multiple isoforms. In the current proteomic analysis of detergent resistant membranes isolated from mouse forebrain two isoforms, the nonmuscle myosins II-B and Va, were unambiguously identified (Tables 1 and 2). Seven peptides were identified for nonmuscle myosin II-B (Table 2). The two highest-ranking tandem mass spectra are depicted in Figure 3A and B, respectively. The peptide tandem mass spectra yielded Mascot scores ranging from 79 to 31 and the total protein score was 398.

The identification of nonmuscle myosin Va is based on two “high confident” peptide identifications (Table 2), the respective tandem mass spectra of which are shown in Figure 4 (panels A and B). The ESI MS/MS spectrum of the doubly protonated peptide ion, LTNLEGVYNSETEK (m/z 798.2), displayed an uninterrupted y -fragment ion series ranging from y_5 to y_{12} allowing the identification of this peptide as the partial sequence 950 – 963 of myosin Va (Fig. 4A).

The tandem mass spectrometry of the doubly charged precursor ion at m/z 780.42 led to the identification of this peptide as the partial sequence 196-210 of myosin Va, i.e. VLASNPIMESIGNAK (Fig. 4B). The identification is based on an intense y -fragment ion series ($y_4 - y_{10}$) and two N-terminal fragment ions, b_2 and b_3 . In addition, contributing to the high confidence identification of this peptide, the y_{10} and the $y_{10} (2+)$ are predominating this fragment ion spectrum; the proline residue at position 6 in this peptide induces preferential cleavage of the backbone amide bond between residue 5 (N) and 6 (P). Oxidation of the methionine residue is confirmed by the neutral loss of CH_3SOH ($\Delta m = 64$ Da) from the fragment ions y_{10} , y_9 and y_8 . Also, the doubly charged y -fragment ion at m/z 538.2, $y_{10} (2+)$, shows loss of CH_3SOH ($\Delta m = 32$ Da). This fragment ion spectrum obtained a score of 67 (Table 2).

Although other nonmuscle class II and class V myosins (IIA, IIC and Vc) have been identified as components of the postsynaptic proteome (Collins et al. 2006),

these particular isoforms were not detected in this analysis. It should be noted, however, that the absence of protein in a proteomic study does not mean necessarily that the protein is not present in the protein preparation rather it indicates the limitation of current approach if complex protein mixtures with wide dynamic ranges are studied. Taken together, these findings indicate that some class II and class V myosin motors are components of a raft-associated membrane skeleton derived from forebrain. As such, some myosin isoforms may be situated in close proximity to either plasma- or endo- membranes and not necessarily reside solely within the PSD of an excitatory synapse.

Verification of raft-associated myosin motors.

We used immunoblot analysis to verify the association of nonmuscle myosin IIB and myosin Va with Triton-X-100-resistant membranes. Both myosin isoforms co-purified with the raft-associated marker caveolin in fraction 4 (Fig. 5A), also identified as the raft fraction on the basis of peak cholesterol concentration (Fig 5B). As in previous analyses, transferrin receptor was excluded from the buoyant raft fraction and located in dense fractions towards the bottom of the sucrose gradient (Fig. 5, fraction 4). As we employed a more aggressive detergent-extraction protocol than had previously been used to study postsynaptic proteins (Hering et al. 2003), we probed fractions for the presence of glutamate receptor subunits to determine if they remained resistant to extraction in 1% Triton X-100. We saw no evidence however, for differential sensitivity between glutamate receptor subunits and myosin motors to 1% Triton X-100. Strong immunoreactive signals for NR1 and GluR2/GluR3 subunits in low-density fractions confirmed the presence of NMDA and AMPA-type glutamate receptor subunits, respectively (Fig 5A). Direct binding partners of NMDA receptor subunits were also detected in lipid raft fractions, providing insight into the spatial orientation of glutamate receptor-associated proteins at membranes. Immunoblot analysis revealed the presence of alpha-actinin-2 (Fig 5A), an actin-binding protein that interacts directly with NMDA receptor subunits, as well as PSD-95, which contains an N-terminal palmitoylation motif that serves to target this scaffolding protein to lipid domains (Craven et al. 1999).

Thus, our findings are in agreement with previous studies that have documented the presence of glutamate receptor subunits in lipid rafts. We also find, however, that lipid raft fractions isolated by flotation in cold 1% Triton X-100 are associated with a number of cytoskeletal, scaffolding and motor proteins. By analogy to other cell types, these proteins could be considered components of a submembrane skeleton.

Myosin IIB is an ATP-sensitive component of postsynaptic density fractions.

We used a second biochemical technique based upon detergent extraction to determine if myosins II-B and myosin Va are differentially expressed in PSD fractions. Although structurally distinct, class II and class V myosins are similar in that they bind to actin filaments via the globular head region of their respective heavy chains. The direct interaction of actin with the myosin head occurs in a cyclical manner that is regulated by ATP and commonly known as the actomyosin ATPase cycle (Geeves et al. 2005). We reasoned that the ATP status of a tissue homogenate could influence formation of an actin-bound myosin complex (i.e actomyosin) and, in turn, the likelihood of myosins being detected in PSD fractions. Preliminary studies revealed the presence of both myosin II-B and myosin Va in purified synaptic membranes and PSD fractions prepared using standard techniques from the forebrain (Fig. 6, upper panels). Although present in brain (Kawamoto and Adelstein 1991), nonmuscle myosin II-A was not detected in these preparations and was likely below the limit of detection used in the comparison (data not shown).

Heavy chains corresponding to myosin II-B and myosin Va were enriched in PSD fractions extracted once (Fig.6, lane 3) and twice (lane 4) with 0.5% Triton X-100, relative to purified synaptic membranes (Fig.6, lane 2). Both myosins were, however, depleted in the PSD III fraction following exposure to 3% sarcosyl (Fig.6, lane 5). This was in contrast to postsynaptic density protein of 95 kDa (PSD-95), a major scaffolding protein of the PSD that was successively enriched in the PSD III fraction and thus served as a positive control for the biochemical

isolation of the fractions (Fig.6, lower panel, lane 5). Throughout these studies, an additional immunoreactive band was observed above the predicted size of myosin Va heavy chain (\approx 200 kDa). This immunoreactive signal appeared to be related to protein concentration and abundance of myosin V in the sample (note upper band in lanes 1 and 4 for myosin Va in Fig. 6), and likely reflects an inability of myosin Va to migrate in the gel at high protein concentrations.

To determine if myosins remain resistant to detergent extraction under conditions that do not favor formation of an actomyosin complex, we prepared PSD I fractions in the presence or absence of exogenously added ATP. Immunoblot analysis of these samples revealed a striking difference between myosin II-B and myosin Va (Fig. 7). Relatively weak immunoreactivity corresponding to myosin II-B heavy chain was observed in fractions prepared in the presence of ATP, whereas myosin II-B remained enriched in PSD I fractions relative to synaptic membranes when prepared under standard conditions (Fig 7, compare lanes 3 and 4). In contrast, a strong immunoreactive signal corresponding to myosin Va heavy chain was detected in PSD I fractions prepared with and without added ATP (Fig 7, compare lanes 3 and 4). Similar immunoblot analyses revealed that actin, alpha-actinin-2, PSD-95 and NMDA receptor subunits NR1 and NR2B were also retained in the PSD I fraction in the presence of added ATP (Fig. 7). Synaptophysin, a presynaptic protein, was absent in both PSD I fractions and thus served to validate the overall purity of the PSD I sample (Fig 7, compare lanes 3 and 4). These findings indicate that myosin II-B can be depleted from PSD fractions extracted once with Triton X-100 if the ATP status of the tissue homogenate is enhanced. This depletion presumably occurs because myosin II-B is weakly associated with the actin cytoskeleton under these experimental conditions. In contrast, the ATP status of the tissue homogenate did not influence our ability to detect myosin Va, NMDA receptor subunits, actin, and NMDA receptor-interacting proteins such as PSD-95 and alpha-actinin-2. These core PSD proteins remained tightly associated with the cytoskeleton and resistant to detergent extraction.

Discussion

Multiple members of the myosin superfamily have been identified as components of postsynaptic excitatory synapses (Cheng et al. 2006; Collins et al. 2006), yet the functional significance of this observation is not fully appreciated. As protein-protein and lipid-protein interactions form the basis of signaling cascades at the membrane, the location of a protein relative to others can be a useful starting point in understanding the overall organization of a protein network. Immunoelectron microscopy of dendritic spines has in fact revealed a striking laminar arrangement of proteins relative to the plasma membrane (Valtschanoff and Weinberg 2001), and a lateral arrangement of proteins in the membrane relative to the PSD (Racz et al. 2004). In the present study, we took advantage of established biochemical techniques based upon Triton-extraction to determine if class II and class V myosin motors were differentially associated with the membrane skeleton and PSD. A proteomic analysis of the major components of detergent-resistant buoyant fractions revealed the presence of both myosin II-B and myosin Va heavy chains with established raft markers. These myosin isoforms were also detected as components of isolated PSD fractions, however myosin II-B appears not to be a core PSD protein. In contrast to myosin Va, myosin II-B is associated with the PSD fraction only when ATP levels are reduced. Together these observations suggest that myosin II-B is loosely associated with the actin cytoskeleton, relative to myosin Va, but that both these molecular motors are in close proximity to membranes.

The identification of nonmuscle myosin II-B as a raft-associated protein was not surprising inasmuch as class II myosins have previously been identified as components of the membrane skeleton. A proteomic analysis of Triton X-100-resistant neutrophil membranes revealed the presence of heavy chains corresponding to myosin II-A and myosin I-G (Nebl et al. 2002). These myosin isoforms remained tightly associated with detergent-resistant membranes even after extraction of all detectable actin and alpha-actinin-2 with 0.1M sodium carbonate (Nebl et al. 2002). The reported actin-independent association of

some myosin isoforms with membranes is strengthened by the fact that class I and class II myosins bind directly to membrane lipids (Adams and Pollard 1989; Li et al. 1994; Murakami et al. 1994; Murakami et al. 1995). In the case of nonmuscle myosin II-A and II-B isoforms, this interaction appears to be with acidic phospholipids such as phosphatidylserine (PS) and phosphatidylinositol (PI) via the tail region of the myosin heavy chain (Murakami et al. 1994; Murakami et al. 1995). Taken together, these observations offer some insight into the possible orientation of myosin II-B relative to the excitatory postsynaptic membrane. It is feasible that myosin II-B can adopt a conformation where it is anchored via its tail region to the inside of the plasma membrane with the head region (which contains the actin-binding domain) pointing towards the underlying actin cytoskeleton. A similar orientation has been proposed in neutrophils, where lipid-bound myosins may relay movements at the plasma membrane to cortical F-actin (Nebl et al. 2002). Although there is physical (Husi et al. 2000; Amparan et al. 2005; Collins et al. 2006) and functional evidence (Lei et al. 2001) for a close association of myosin II-B with the NMDA-type glutamate receptor, a general role for myosin II-B as a component of the submembrane skeleton is also consistent with recent studies that indicate myosin II-B is a key regulator of spine morphology (Ryu et al. 2006). Treatment of hippocampal neurons with the specific myosin II inhibitor (+) blebbistatin, or knockdown of endogenous myosin II-B by RNA interference, caused marked changes in the size and shape of dendritic spines (Straight et al. 2003; Ryu et al. 2006). Blebbistatin treatment also reduced excitatory postsynaptic currents (EPSCs) in hippocampal slice preparations, indicating that a functional myosin II complex is required for normal excitatory transmission (Ryu et al. 2006).

Our proteomic analysis of major raft-associated proteins also confirmed the presence of myosin Va as a component of the submembrane skeleton. Myosin Va has been repeatedly identified as a component of the postsynaptic proteome and is thought to serve a trafficking function at the synapse (Naisbitt et al. 2000; Walikonis et al. 2000; Bridgman 2004; Collins et al. 2006). The myosin V complex is composed of two heavy chains which each bind multiple calmodulins,

two myosin essential light chains and one dynein light chain (LC8) (Espindola et al. 2000). Much attention has focused on LC8, as this protein has been shown to bind directly to guanylate kinase domain-associated protein (GKAP) (Naisbitt et al. 2000) that, in turn, binds to PSD-95 (Naisbitt et al. 1997). It has been noted that LC8 has a wide distribution throughout the dendritic spine, consistent with a potential trafficking function whereby LC8 may serve to couple “cargo” to a myosin V motor (Valtschanoff and Weinberg 2001). However, Valtschanoff and Weinberg (2001) also noted that LC8 was concentrated at the postsynaptic plasma membrane. It is important to note that LC8 is present in all functional dynein motor complexes and interacts with many other proteins (Jaffrey and Snyder 1996; Puthalakath et al. 1999; Schnorrer et al. 2000; Kaiser et al. 2003). Nevertheless, our identification of myosin Va as a raft-associated protein is consistent with the localization of one of its known light chains, LC8, at the plasma membrane (Valtschanoff and Weinberg 2001). The exact role of myosin Va, however, remains unclear as the *dilute-lethal* mouse which is a spontaneous myosin Va mutant, displays a normal glutamate receptor distribution and normal hippocampal physiology (Petralia et al. 2001; Schnell and Nicoll 2001). As at least two other nonmuscle myosin V isoforms (Vb and Vc) are present at glutamatergic synapses, it is possible that these isoforms, or even other classes of myosin, may compensate for the loss of Va in this animal (Collins et al. 2006; Lise et al. 2006).

Myosin II-B could be depleted from standard PSD I fractions by supplementing the tissue homogenate with ATP. Myosin Va, however, was unaffected by this treatment presumably as a result of its ability to form a detergent-resistant actomyosin V complex. These findings are consistent with structural and enzymatic studies that indicate the affinity of myosin V for actin is relatively high, and that it can remain associated with actin even in the presence of ATP (Vale 2003). The observed difference in ATP sensitivity between myosin II-B and myosin Va isoforms offers a possible explanation as to why class II myosins have generally been detected far less frequently as components of the PSD than myosin Va (Collins et al. 2006). If the ATP status of the tissue remains high

during the generation of postsynaptic fractions, class II myosins may be held in a low-affinity actin binding state and thus be removed by detergent. In theory, myosin II isoforms could also be detected infrequently in PSD fractions if they were less abundant, or more peripherally associated with the PSD. With regard to the location of myosin II-B relative to the PSD, it is significant that in previous immunoelectron microscopy studies, myosin II was found close to the plasma membrane and endomembranes within the spine, with only sparse labeling of the PSD (Morales and Fifkova 1989; Miller et al. 1992). These reports are consistent with a submembrane location of myosin II-B, reported herein, rather than its classification as a core PSD protein.

We used a combination of mass spectrometry and immunoblot analysis to characterize major components of a 1% Triton X-100-resistant raft fraction from forebrain. This subset of the total proteome was represented by raft associated proteins, cytoskeletal proteins, receptors and channels, and mediators of cell adhesion and membrane dynamics, many of which have previously been identified as components of lipid raft fractions from a variety of different preparations (De Matteis and Morrow 2000; Nebl et al. 2002; Ciana et al. 2005). The identification of NR1, AMPA-type subunits and PSD-95 was in agreement with a previous report that identified these proteins as components of 0.5% Triton X-100-resistant membrane preparations from whole rat brain (Hering et al. 2003). As we isolated a heterogeneous detergent-resistant membrane fraction, it is not possible to determine if the proteins that we identified are associated with the same lipid raft. However, the identification of glutamate receptor subunits and associated proteins such as PSD-95, CaMKinase II subunits, src, MARCKS, homer 1, dynamin-2 and alpha-actinin-2 following the more stringent extraction conditions employed in the present study is consistent with the view that specialized membrane domains are intimately associated with the underlying cytoskeleton to coordinate glutamatergic signal transduction.

In summary, the postsynaptic proteome appears to be represented by a series of overlapping populations of proteins and has been described as one of the most

complicated subcellular structures in eukaryotic cells (Collins et al. 2006). The region of the postsynaptic membrane adjacent to the PSD represents a relatively small percentage of the total surface area of the neuronal plasma membrane (Sorra and Harris 2000). Thus, our characterization of a buoyant density lipid raft fraction provides some insight into proteins that may be found close to plasma and endomembranes in forebrain. This technique provides a complementary approach to previous proteomic analyses of PSD fractions and receptor-associated complexes and adds to our overall understanding of the spatial organization of myosin II-B and Va at synapses.

Figure legends

Figure 1. Characterization of a detergent-resistant lipid raft fraction from mouse forebrain. **A.** Orientation of fractions extracted in 1% Triton X-100 from mouse forebrain following buoyant-density gradient. **B.** Graph depicting cholesterol (closed squares) and protein content (open circles) of fractions extracted in 1% Triton X-100 from mouse forebrain from a representative buoyant-density sucrose gradient repeated more than eight times with similar results. **C.** Immunoblot analysis of fractions 1 to 11 reveals the presence of caveolin in the cholesterol-rich fraction number 4, whereas transferrin (TfR) receptor is located in high density, protein-rich fractions. **Methods.** Mouse forebrain was homogenized in a buffer containing 320 mM sucrose, 25mM HEPES, 2mM sodium orthovanadate, 1mM sodium fluoride pH 7.4, plus protease inhibitors and centrifuged at 800 x g, for 10 minutes at 4°C to pellet nuclei. The resulting supernatant was pelleted by centrifugation and resuspended in a buffer containing 1% Triton X-100 in 25 mM Hepes, 1mM EDTA plus protease inhibitors (pH 7.4) with rotation for 1 hour at 4 °C. The brain extract was then transferred to a centrifuge tube, mixed with an equal volume of 90% sucrose, and overlaid with 35%, 25%, 15% and 5% sucrose all containing 1% Triton X-100. After centrifugation at 230,000 x g for at 24 hours at 4 °C, equal volumes of each fraction were assayed for cholesterol, total protein, caveolin and transferrin (TfR) receptor.

Figure 2. Coomassie blue stain of control and detergent-resistant lipid raft fractions extracted in 1% Triton X-100 from mouse forebrain following three independent buoyant-density gradients. Proteins were resolved by PAGE in 4-12% gradient gels and stained to reveal proteins in control (fraction 1, lane 2) and lipid raft fractions (fraction 4, lanes 3 to 5). Fractions 1a and 4a are taken from the same buoyant-density gradient (gradient a). Fractions 4b and 4c are derived from two additional buoyant-density gradients (b and c, respectively). Fraction 4c was concentrated approximately four-fold using an Ultrafree-0.5

centrifugal filter device (Millipore, Billerica, MA), to highlight eight prominent bands and a gel region that were excised for tandem mass spectrometry.

Figure 3. Tandem mass spectrometric identification of nonmuscle myosin II-B. **A.** Tandem mass spectrum of the peptide IGQLEEQLEQEAK (aa 1823 - 1835). The spectrum was obtained from the precursor ion (P) at m/z 757.9, the doubly protonated peptide $[M+2H]^{2+}$. An intense y -fragment ion series (y_4 - y_{10} and y_{12}) was observed. This spectrum obtained a score of 79. **B.** Tandem mass spectrum of the peptide QLEEAEEEEATR (aa 1885 – 1895). The precursor ion (P) at m/z 652.81 (2+) was subjected to MS/MS analysis. This spectrum is dominated by a complete y -ion series (up to y_{10}) and yielded a score of 75. The asterisks * indicate loss of H_2O ($\Delta m = 18$ Da) from the respective y -ion.

Figure 4. Tandem mass spectrometric identification of nonmuscle myosin Va. **A.** ESI MS/MS spectrum of the doubly protonated peptide ion at m/z 798.2 which resulted in the identification of the peptide LTNLEGVYNSETEK, the partial sequence 950 – 963 of nonmuscle myosin Va (MYO5A_MOUSE). The spectrum is dominated by y -fragment ions ranging from y_5 to y_{12} . Ions annotated with * indicate neutral loss of H_2O . The precursor ion is marked with “P”. This spectrum obtained a score of 56. **B.** Tandem mass spectrum of the precursor ion “P” at m/z 780.42 (2+). The spectrum led to the identification of the peptide encompassing the partial sequence aa 196 - 210 of nonmuscle myosin Va, VLASNPIMESIGNAK. Beside the the two N-terminal fragment ions b_2 and b_3 the spectrum shows an uninterrupted y -fragment ion series (y_4 - y_{10}). Oxidation of the methionine residue is confirmed by the neutral loss of CH_3SOH ($\Delta m = 64$ Da) from the fragment ions y_{10} , y_9 and y_8 . Also, the doubly charged y -fragment ion at m/z 538.2, y_{10} (2+), shows loss of CH_3SOH ($\Delta m = 32$ Da). Ions that resulted from loss of CH_3SOH are marked with #. The predominance of the y_{10} and the y_{10} (2+) ion is caused by the presence of the proline residue at position 6. This MS/MS spectrum obtained a score of 67.

Figure 5. Myosins IIB and Va co-purify with lipid raft fractions. **A.** Immunoblot analysis of fractions extracted in 1% Triton X-100 from mouse forebrain following buoyant-density sucrose gradient. **B.** Graph depicting cholesterol and protein content of the gradient described in A. **Methods.** Gradients were prepared from mouse forebrain as described in Materials and methods. Equal volumes of each fraction were analyzed by immunoblot analysis for caveolin, myosin IIB, myosin Va, the NR1 subunit of the NMDA receptor, alpha-actinin-2, PSD-95, GluR subunits 2/3 and transferrin (TfR) receptor. Equal volumes of each fraction were also assayed for cholesterol and total protein content.

Figure 6. Myosin IIB and myosin Va are enriched in postsynaptic density fractions. Immunoblot analysis reveals significant enrichment of heavy chains corresponding to myosin IIB and myosin Va in postsynaptic density fractions when compared with purified synaptic membranes. Purified synaptic membranes (lanes 1 and 2) were purified by discontinuous sucrose density-gradient from rat forebrain (Carlin et al. 1980), and postsynaptic density fractions isolated according to the method of Cho and coworkers (Cho et al. 1992), resulting in: PSD I (lane 3), PSD II (lane 4) and PSD III (lane 5). Immunoreactive bands corresponding to myosin IIB, myosin Va and PSD-95 are detected in lane 1 (30 μ g). Equal concentrations (3 μ g) of synaptosomes and PSD fractions were loaded in lanes 2 to 5. Myosin IIB and myosin Va are enriched in PSD II (compare lane 4 to lane 2), but depleted in PSD III (lane 5). PSD-95 is enriched in successive detergent extracted PSD fractions and serves as a control.

Figure 7. Retention of myosin IIB in the postsynaptic density fraction is influenced by the presence of ATP. Immunoblot analysis reveals that myosin IIB (upper panel) is depleted from the PSD I fraction if the extract buffer is supplemented with ATP (10 mM). Detection of myosin Va, actin, alpha-actinin-2,

PSD-95, NR1 and NR2B subunits is not altered by the presence of ATP (10 mM). Immunoreactive bands corresponding to major postsynaptic proteins are detected in purified synaptic membranes which were loaded in lanes 1 (30 μ g) and 2 (3 μ g). Postsynaptic density fractions (3 μ g) prepared in the absence and presence of ATP (10 mM) were loaded in lanes 3 and 4, respectively. Synaptophysin, a presynaptic protein, was not detected in postsynaptic density fractions (lanes 3 and 4) and serves as a control.

Acknowledgments

The authors thank Brian Arbogast and Gaurav Bajaj for excellent technical assistance, and Dr. Baltz Frei of the OSU Linus Pauling Institute for the use of his GeminiXS microplate spectrofluorometer. This work was supported by an award from the American Association of Colleges of Pharmacy (AACP) New Investigator Program (NIP), supported by the American Foundation for Pharmaceutical Education (ACPE) to J.I. and the Mass Spectrometry and Macromolecular Structure & Interactions (C.M.) Facilities and Services Cores of Grant ES000210 from the National Institute of Environmental Health Sciences.

Supplementary Material

Table S1. 'Tentatively identified' proteins found in the lipid raft fraction (i.e. fraction 4).

References

- Adams R. J. and Pollard T. D. (1989) Binding of myosin I to membrane lipids. *Nature* **340**, 565-568.
- Amparan D., Avram D., Thomas C. G., Lindahl M. G., Yang J., Bajaj G. and Ishmael J. E. (2005) Direct interaction of myosin regulatory light chain with the NMDA receptor. *J Neurochem* **92**, 349-361.
- Bae T. J., Kim M. S., Kim J. W., Kim B. W., Choo H. J., Lee J. W., Kim K. B., Lee C. S., Kim J. H., Chang S. Y., Kang C. Y., Lee S. W. and Ko Y. G. (2004) Lipid raft proteome reveals ATP synthase complex in the cell surface. *Proteomics* **4**, 3536-3548.
- Biemann K. (1988) Contributions of mass spectrometry to peptide and protein structure. *Biomed Environ Mass Spectrom* **16**, 99-111.
- Bridgman P. C. (2004) Myosin-dependent transport in neurons. *J Neurobiol* **58**, 164-174.
- Carlin R. K., Grab D. J., Cohen R. S. and Siekevitz P. (1980) Isolation and characterization of postsynaptic densities from various brain regions: enrichment of different types of postsynaptic densities. *J Cell Biol* **86**, 831-845.
- Cheng D., Hoogenraad C. C., Rush J., Ramm E., Schlager M. A., Duong D. M., Xu P., Wijayawardana S. R., Hanfelt J., Nakagawa T., Sheng M. and Peng J. (2006) Relative and absolute quantification of postsynaptic density proteome isolated from rat forebrain and cerebellum. *Mol Cell Proteomics* **5**, 1158-1170.
- Cho K. O., Hunt C. A. and Kennedy M. B. (1992) The rat brain postsynaptic density fraction contains a homolog of the Drosophila discs-large tumor suppressor protein. *Neuron* **9**, 929-942.
- Ciana A., Balduini C. and Minetti G. (2005) Detergent-resistant membranes in human erythrocytes and their connection to the membrane-skeleton. *J Biosci* **30**, 317-328.
- Collins M. O., Husi H., Yu L., Brandon J. M., Anderson C. N., Blackstock W. P., Choudhary J. S. and Grant S. G. (2006) Molecular characterization and comparison of the components and multiprotein complexes in the postsynaptic proteome. *J Neurochem* **97 Suppl 1**, 16-23.
- Craven S. E., El-Husseini A. E. and Brecht D. S. (1999) Synaptic targeting of the postsynaptic density protein PSD-95 mediated by lipid and protein motifs. *Neuron* **22**, 497-509.
- De Matteis M. A. and Morrow J. S. (2000) Spectrin tethers and mesh in the biosynthetic pathway. *J Cell Sci* **113 (Pt 13)**, 2331-2343.
- Espindola F. S., Suter D. M., Partata L. B., Cao T., Wolenski J. S., Cheney R. E., King S. M. and Mooseker M. S. (2000) The light chain composition of chicken brain myosin-Va: calmodulin, myosin-II essential light chains, and 8-kDa dynein light chain/PIN. *Cell Motil Cytoskeleton* **47**, 269-281.

- Geeves M. A., Fedorov R. and Manstein D. J. (2005) Molecular mechanism of actomyosin-based motility. *Cell Mol Life Sci* **62**, 1462-1477.
- Harder T. and Simons K. (1997) Caveolae, DIGs, and the dynamics of sphingolipid-cholesterol microdomains. *Curr Opin Cell Biol* **9**, 534-542.
- Harris K. M. and Kater S. B. (1994) Dendritic spines: cellular specializations imparting both stability and flexibility to synaptic function. *Annu Rev Neurosci* **17**, 341-371.
- Hering H., Lin C. C. and Sheng M. (2003) Lipid rafts in the maintenance of synapses, dendritic spines, and surface AMPA receptor stability. *J Neurosci* **23**, 3262-3271.
- Husi H., Ward M. A., Choudhary J. S., Blackstock W. P. and Grant S. G. (2000) Proteomic analysis of NMDA receptor-adhesion protein signaling complexes. *Nat Neurosci* **3**, 661-669.
- Jaffrey S. R. and Snyder S. H. (1996) PIN: an associated protein inhibitor of neuronal nitric oxide synthase. *Science* **274**, 774-777.
- Kaiser F. J., Tavassoli K., Van den Bemd G. J., Chang G. T., Horsthemke B., Moroy T. and Ludecke H. J. (2003) Nuclear interaction of the dynein light chain LC8a with the TRPS1 transcription factor suppresses the transcriptional repression activity of TRPS1. *Hum Mol Genet* **12**, 1349-1358.
- Kawamoto S. and Adelstein R. S. (1991) Chicken nonmuscle myosin heavy chains: differential expression of two mRNAs and evidence for two different polypeptides. *J Cell Biol* **112**, 915-924.
- Kennedy M. B. (1998) Signal transduction molecules at the glutamatergic postsynaptic membrane. *Brain Res Brain Res Rev* **26**, 243-257.
- Kornau H. C., Schenker L. T., Kennedy M. B. and Seeburg P. H. (1995) Domain interaction between NMDA receptor subunits and the postsynaptic density protein PSD-95. *Science* **269**, 1737-1740.
- Lei S., Czerwinska E., Czerwinski W., Walsh M. P. and MacDonald J. F. (2001) Regulation of NMDA receptor activity by F-actin and myosin light chain kinase. *J Neurosci* **21**, 8464-8472.
- Li D., Miller M. and Chantler P. D. (1994) Association of a cellular myosin II with anionic phospholipids and the neuronal plasma membrane. *Proc Natl Acad Sci U S A* **91**, 853-857.
- Li N., Shaw A. R., Zhang N., Mak A. and Li L. (2004) Lipid raft proteomics: analysis of in-solution digest of sodium dodecyl sulfate-solubilized lipid raft proteins by liquid chromatography-matrix-assisted laser desorption/ionization tandem mass spectrometry. *Proteomics* **4**, 3156-3166.
- Lise M. F., Wong T. P., Trinh A., Hines R. M., Liu L., Kang R., Hines D. J., Lu J., Goldenring J. R., Wang Y. T. and El-Husseini A. (2006) Involvement of myosin Vb in glutamate receptor trafficking. *J Biol Chem* **281**, 3669-3678.

- Lowry O. H., Rosebrough N. J., Farr A. L. and Randall R. J. (1951) Protein measurement with the Folin phenol reagent. *J Biol Chem* **193**, 265-275.
- Miller M., Bower E., Levitt P., Li D. and Chantler P. D. (1992) Myosin II distribution in neurons is consistent with a role in growth cone motility but not synaptic vesicle mobilization. *Neuron* **8**, 25-44.
- Morales M. and Fifkova E. (1989) In situ localization of myosin and actin in dendritic spines with the immunogold technique. *J Comp Neurol* **279**, 666-674.
- Murakami N., Elzinga M., Singh S. S. and Chauhan V. P. (1994) Direct binding of myosin II to phospholipid vesicles via tail regions and phosphorylation of the heavy chains by protein kinase C. *J Biol Chem* **269**, 16082-16090.
- Murakami N., Singh S. S., Chauhan V. P. and Elzinga M. (1995) Phospholipid binding, phosphorylation by protein kinase C, and filament assembly of the COOH terminal heavy chain fragments of nonmuscle myosin II isoforms MIIA and MIIIB. *Biochemistry* **34**, 16046-16055.
- Naisbitt S., Kim E., Weinberg R. J., Rao A., Yang F. C., Craig A. M. and Sheng M. (1997) Characterization of guanylate kinase-associated protein, a postsynaptic density protein at excitatory synapses that interacts directly with postsynaptic density-95/synapse-associated protein 90. *J Neurosci* **17**, 5687-5696.
- Naisbitt S., Valtschanoff J., Allison D. W., Sala C., Kim E., Craig A. M., Weinberg R. J. and Sheng M. (2000) Interaction of the postsynaptic density-95/guanylate kinase domain-associated protein complex with a light chain of myosin-V and dynein. *J Neurosci* **20**, 4524-4534.
- Nebi T., Pestonjamas K. N., Leszyk J. D., Crowley J. L., Oh S. W. and Luna E. J. (2002) Proteomic analysis of a detergent-resistant membrane skeleton from neutrophil plasma membranes. *J Biol Chem* **277**, 43399-43409.
- Petralia R. S., Wang Y. X., Sans N., Worley P. F., Hammer J. A., 3rd and Wenthold R. J. (2001) Glutamate receptor targeting in the postsynaptic spine involves mechanisms that are independent of myosin Va. *Eur J Neurosci* **13**, 1722-1732.
- Pike L. J. (2004) Lipid rafts: heterogeneity on the high seas. *Biochem J* **378**, 281-292.
- Puthalakath H., Huang D. C., O'Reilly L. A., King S. M. and Strasser A. (1999) The proapoptotic activity of the Bcl-2 family member Bim is regulated by interaction with the dynein motor complex. *Mol Cell* **3**, 287-296.
- Racz B., Blanpied T. A., Ehlers M. D. and Weinberg R. J. (2004) Lateral organization of endocytic machinery in dendritic spines. *Nat Neurosci* **7**, 917-918.
- Rodgers W. and Zavzavadjian J. (2001) Glycolipid-enriched membrane domains are assembled into membrane patches by associating with the actin cytoskeleton. *Exp Cell Res* **267**, 173-183.

- Ryu J., Liu L., Wong T. P., Wu D. C., Burette A., Weinberg R., Wang Y. T. and Sheng M. (2006) A critical role for Myosin IIb in dendritic spine morphology and synaptic function. *Neuron* **49**, 175-182.
- Schnell E. and Nicoll R. A. (2001) Hippocampal synaptic transmission and plasticity are preserved in myosin Va mutant mice. *J Neurophysiol* **85**, 1498-1501.
- Schnorrer F., Bohmann K. and Nusslein-Volhard C. (2000) The molecular motor dynein is involved in targeting swallow and bicoid RNA to the anterior pole of *Drosophila* oocytes. *Nat Cell Biol* **2**, 185-190.
- Sellers J. R. (2000) Myosins: a diverse superfamily. *Biochim Biophys Acta* **1496**, 3-22.
- Sheng M. and Lee S. H. (2000) Growth of the NMDA receptor industrial complex. *Nat Neurosci* **3**, 633-635.
- Sheng M. and Sala C. (2001) PDZ domains and the organization of supramolecular complexes. *Annu Rev Neurosci* **24**, 1-29.
- Sorra K. E. and Harris K. M. (2000) Overview on the structure, composition, function, development, and plasticity of hippocampal dendritic spines. *Hippocampus* **10**, 501-511.
- Straight A. F., Cheung A., Limouze J., Chen I., Westwood N. J., Sellers J. R. and Mitchison T. J. (2003) Dissecting temporal and spatial control of cytokinesis with a myosin II inhibitor. *Science* **299**, 1743-1747.
- Vale R. D. (2003) Myosin V motor proteins: marching stepwise towards a mechanism. *J Cell Biol* **163**, 445-450.
- Valensin S., Paccani S. R., Ulivieri C., Mercati D., Pacini S., Patrussi L., Hirst T., Lupetti P. and Baldari C. T. (2002) F-actin dynamics control segregation of the TCR signaling cascade to clustered lipid rafts. *Eur J Immunol* **32**, 435-446.
- Valtschanoff J. G. and Weinberg R. J. (2001) Laminar organization of the NMDA receptor complex within the postsynaptic density. *J Neurosci* **21**, 1211-1217.
- Walikonis R. S., Jensen O. N., Mann M., Provance D. W., Jr., Mercer J. A. and Kennedy M. B. (2000) Identification of proteins in the postsynaptic density fraction by mass spectrometry. *J Neurosci* **20**, 4069-4080.
- Woehlke G. and Schliwa M. (2000) Walking on two heads: the many talents of kinesin. *Nat Rev Mol Cell Biol* **1**, 50-58.
- Xiao B., Tu J. C., Petralia R. S., Yuan J. P., Doan A., Breder C. D., Ruggiero A., Lanahan A. A., Wenthold R. J. and Worley P. F. (1998) Homer regulates the association of group 1 metabotropic glutamate receptors with multivalent complexes of homer-related, synaptic proteins. *Neuron* **21**, 707-716.

Table 1: Proteins identified as major components of detergent-resistant membranes

Gel Region	Protein	Accession Number	Category	Peptides
1 >250 kD	Spectrin alpha chain, brain (non-erythroid)	P16546	Cytoskeleton Actin	28
	Spectrin beta chain, brain (non-erythroid)	Q62261	Cytoskeleton Actin	26
	Microtubule-associated protein (MAP 2)	P20357	Cytoskeleton other	2
2 >150- 250 kD	Contactin-1 precursor (CNTN1)	P12960	Cell adhesion	10
	Nonmuscle myosin II-B heavy chain (NMHC)	Q61879	Actin-based Motor	7
	Tubulin beta-5 chain	P99024	Cytoskeleton other	6
	Nonmuscle myosin-Va heavy chain (dilute myosin)	Q99104	Actin-based Motor	2
	Lipophilin	P60202	Lipoprotein	2
3 ~130	Contactin-1 precursor (CNTN1)	P12960	Cell adhesion	43
	Neurofilament medium polypeptide (NF-M)	P08553	Cytoskeleton other	23
	Dihydropyridine-sensitive L-type, calcium channel alpha-2/delta subunit	O08532	Receptors and channels	12
	Contactin-2 precursor (TAG-1)	Q61330	Cell adhesion	9
	Laminin alpha-3 chain (Nicein alpha subunit)	Q61789	Cell adhesion	4
	Unc-13 homolog B (Munc13-2)	Q9Z1N9	Exocytosis	3
	Myotubularin-related protein 9	Q9Z2D0	Phosphatase	3
	Angiomotin-like protein 2	Q8K371	Cytoskeleton Actin	3
	RAB6-interacting protein 2 (CAZ-associated structural protein CAST2)	Q99MI1	Cytomatrix Scaffold	2

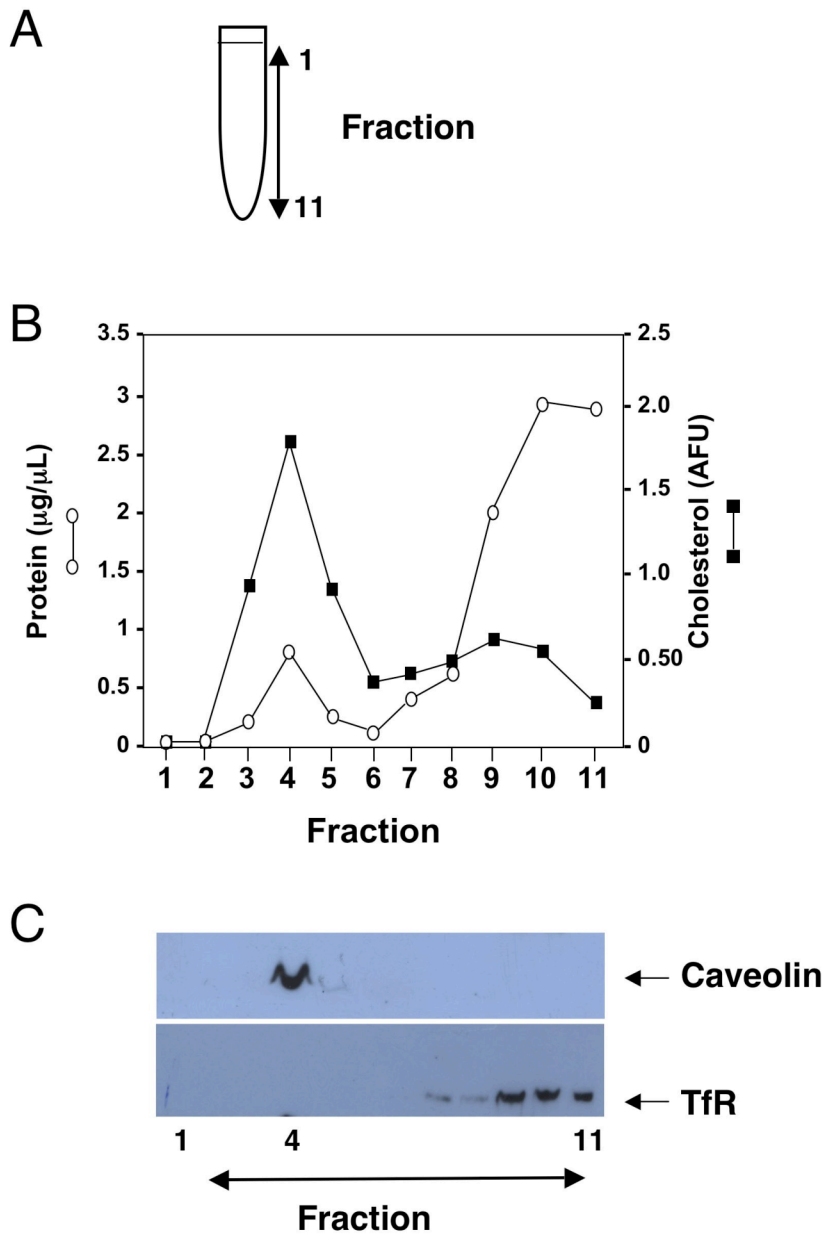
	Dynamin-2	P39054	Endocytosis	2
	Phosphatidylinositol 3-kinase regulatory alpha subunit	P26450	Kinase	2
	Cullin-3 (ubiquitin ligase)	Q9JLV5	Ubiquitination	2
4 < 75 kD	Neurofilament triplet L protein	P08551	Cytoskeleton other	25
	Vacuolar ATP synthase catalytic subunit A	P50516	Receptors and channels	21
	Solute carrier 25 member 1 (Aralar1)	Q8BH59	Mitochondria	3
5 ~60	Alpha-internexin	P46660	Cytoskeleton other	21
	Limbic system-associated membrane protein precursor	Q8BLK3	Cell adhesion	9
	Ca ²⁺ /calmodulin dependent protein kinase II beta	P28652	Kinase	7
	Synapsin-2	Q64332	Membrane dynamics	4
	Synaptotagmin-1	P46096	Membrane dynamics	4
	Vacuolar ATP synthase subunit B, brain isoform	P62814	Receptors and channels	2
	Myristoylated alanine-rich C-kinase substrate (MARCKS)	P26645	Cytoskeleton Actin	2
	Neuronal proto-oncogene tyrosine-protein kinase (c-Src)	P05480	Kinase	2
	Brain acid soluble protein1	Q91XV3	Cytoskeleton other	8
	Tubulin		Cytoskeleton other	
	beta-2 chain	P68372		13
	beta-3 chain	Q9ERD7		11
	beta-4 chain	Q9D6F9		11
beta-1 chain	P69893		10	
beta-6 chain	Q9922F4		9	
alpha-1 chain	P68369		7	
alpha-4 chain	P68368		4	
Ca ²⁺ /calmodulin-dependent protein kinase II alpha	P11275	Kinase	5	

7 <50	Actin beta alpha	P60710 P68033	Cytoskeleton Actin	16 8
	Neuromodulin	P06837	Membrane dynamics	8
	Septin-5 (peanut-like protein)	Q9Z2Q6	Cytoskeleton other	4
	Homer protein homolog 1	Q9Z2Y3	Scaffold	3
	2',3'-cyclic-nucleotide 3'- phosphodiesterase (CNPase)	P16330	Phosphodiesterase	2
8 >37 kD	Guanine nucleotide -binding protein G(o), alpha subunit	P18872	GTPases and Regulators	18
	Guanine nucleotide-binding protein G(z), alpha subunit	O70443	GTPases and Regulators	7
	Guanine nucleotide-binding protein G(i), alpha subunit	P08752	GTPases and Regulators	3
	Vacuolar ATP synthase subunit d	P51863	Receptors and channels	3
9 > 25 kD	Thy-1 membrane glycoprotein precursor	P01831	Cell adhesion	4

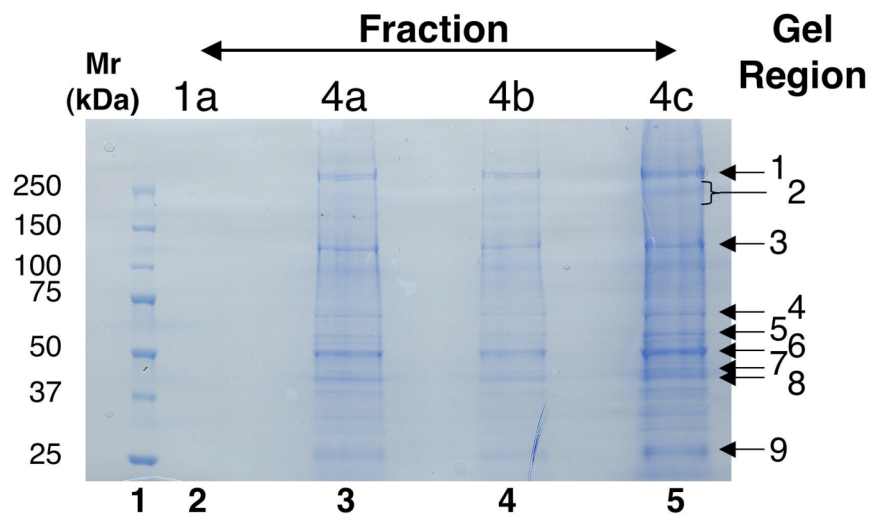
Table 2: Summary of peptides corresponding to myosin heavy chains identified by in-gel digest of region 2 followed by tandem mass spectrometry

Myosin Heavy Chain	Obsd. (m/z) ^a	M _r (expt.)	M _r (calc.)	Δm	Score	Peptide
Nonmuscle myosin II-B (Myosin-10) Mass: 228,855 Protein Score: 380 Queries matched: 7	652.81	1303.61	1303.59	0.02	75	R.QLEEAEEEEATR.A
	659.88	1317.75	1317.74	0.01	65	K.LDPHLVLDQLR.C
	757.89	1513.76	1513.76	-0.00	79	K.IGQLEEQLEQEAKE.E
	824.92	1647.82	1647.83	-0.01	34	R.AVIYNPATQADWTAK.K
	871.99	1741.97	1741.94	0.04	58	R.QLLOANPILESFGNAK.T
	646.65	1936.93	1936.95	-0.02	41	R.LQQELDDLTVDLDHQR.Q
	691.72	2072.15	2072.06	0.08	31	K.LQNELDNVSTLLEEAEEK.G ^b
Nonmuscle myosin Va (Myosin-5a) Mass: 215,459 Protein Score: 123 Queries matched: 2	780.42	1558.83	1558.80	0.03	67	K.VLASNPIMESIGNAK.T + Oxidation (M)
	798.90	1595.78	1595.77	0.01	56	K.LTNLEGVYNSETEK.L

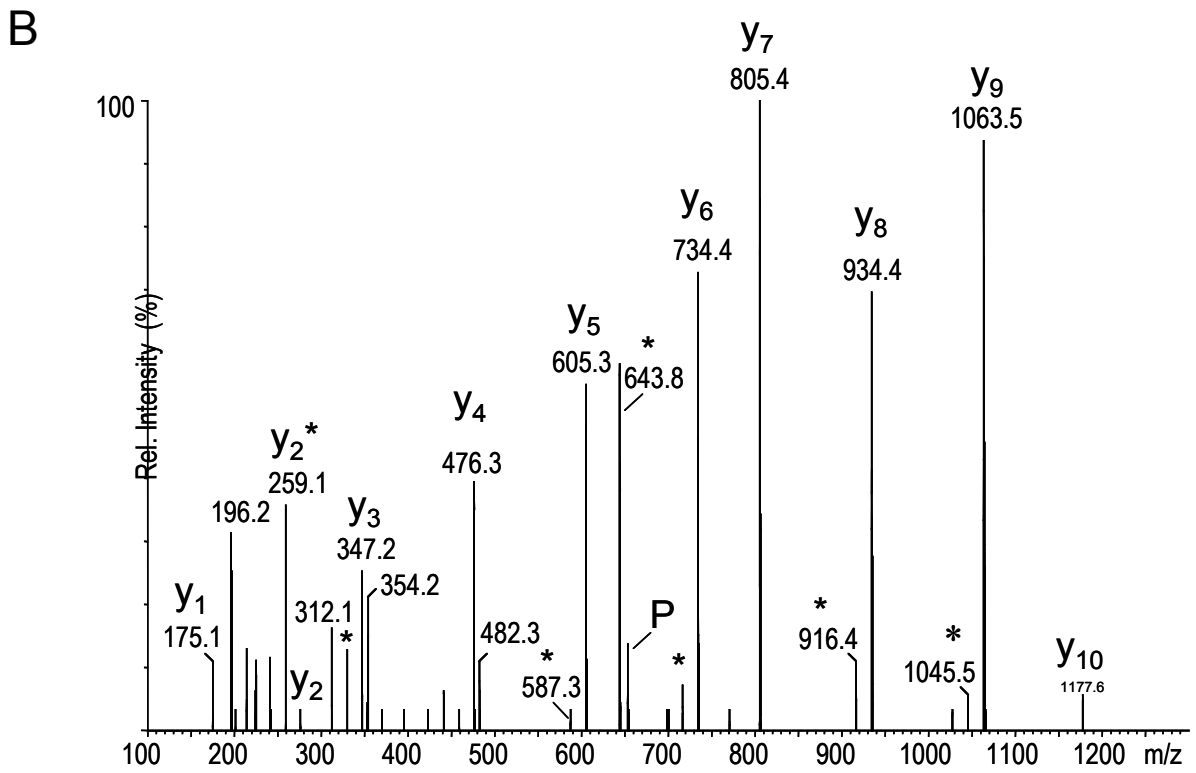
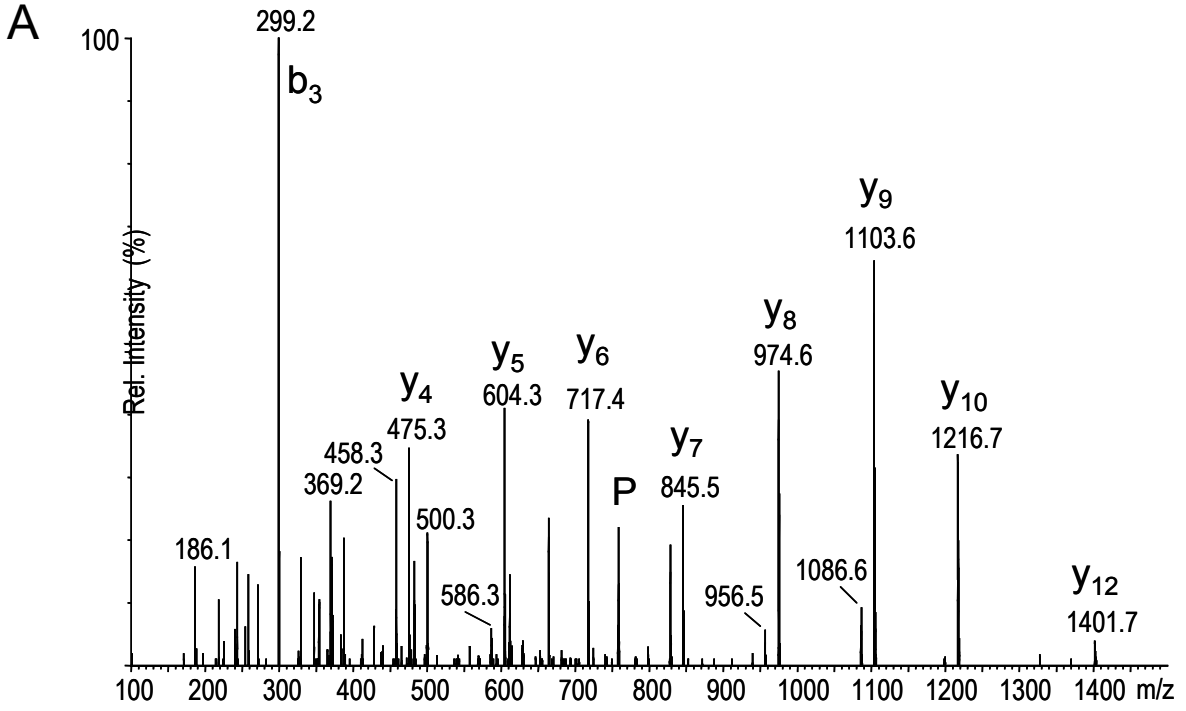
^a doubly charged precursor ions, $[M+2H]^{2+}$, were used for MS/MS experiments; ^b Peptide with one missed trypsin cleavage site.



Ishmael et al. Figure 2

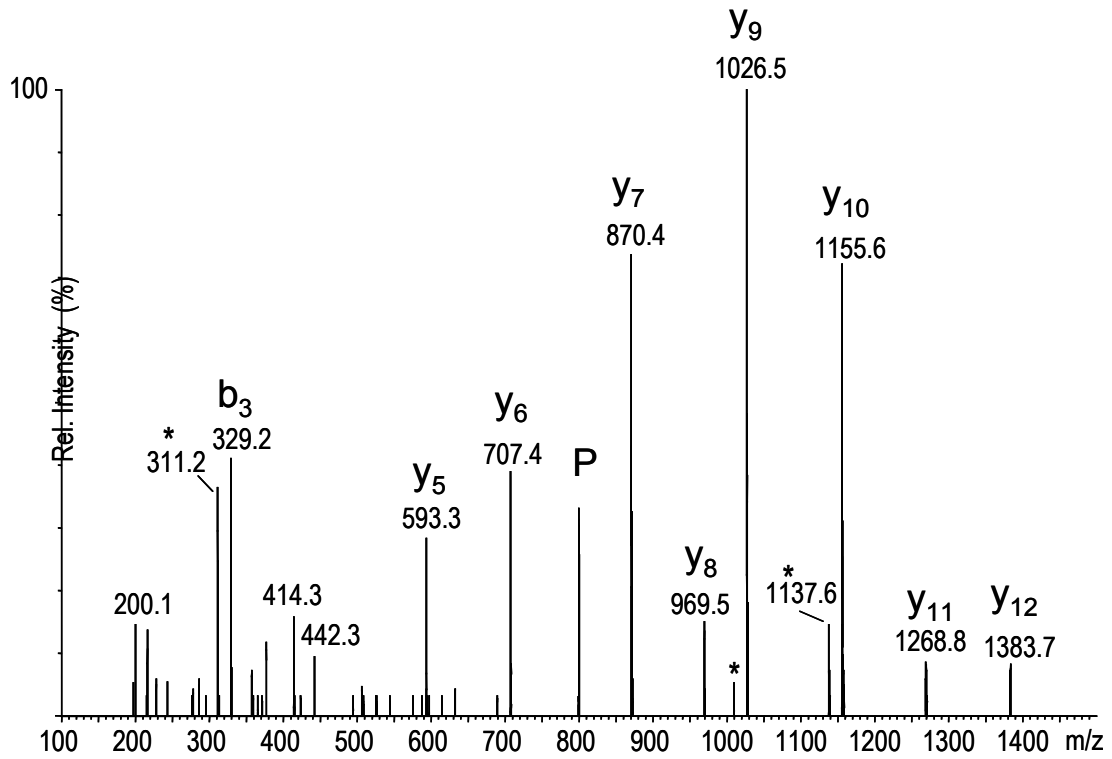


Ishmael et al. Figure 3.

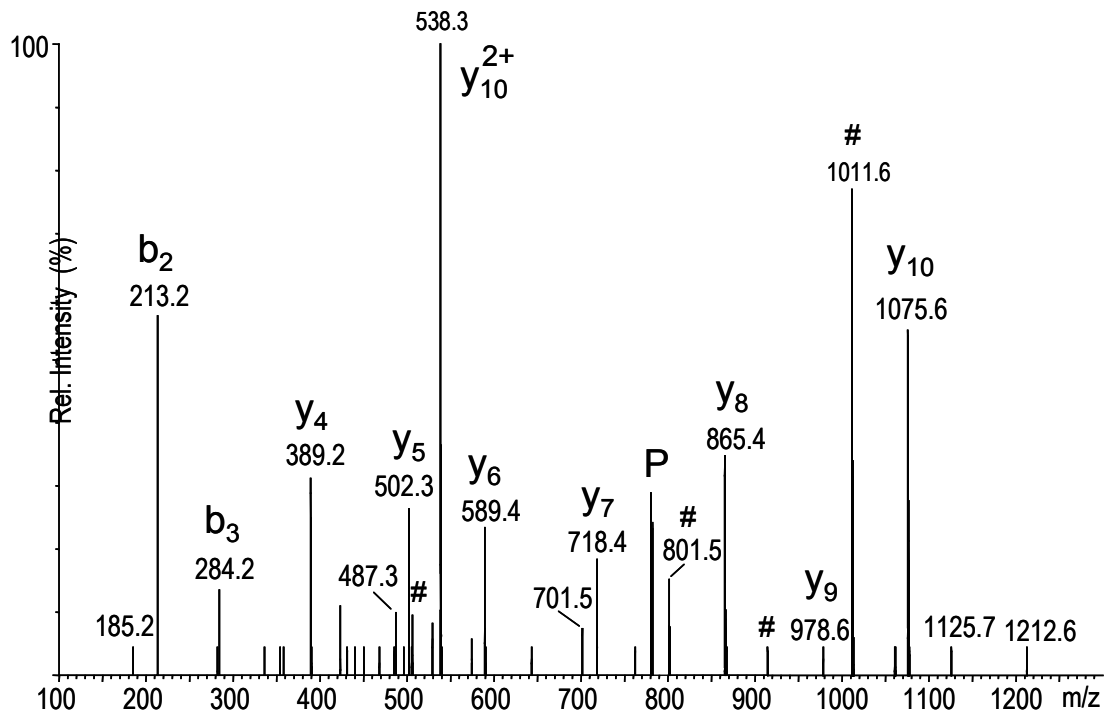


Ishmael et al. Figure 4.

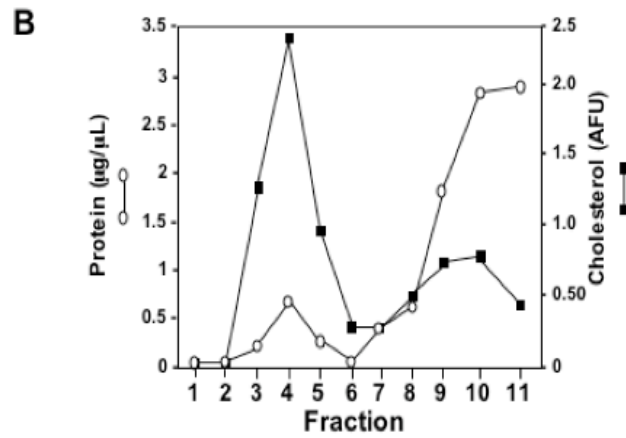
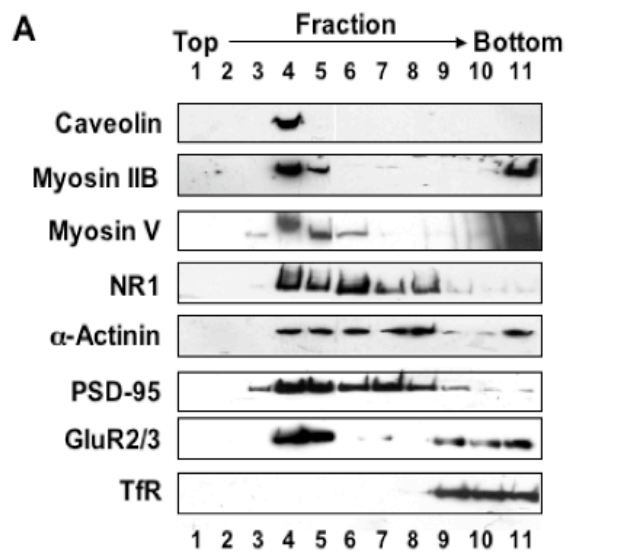
A



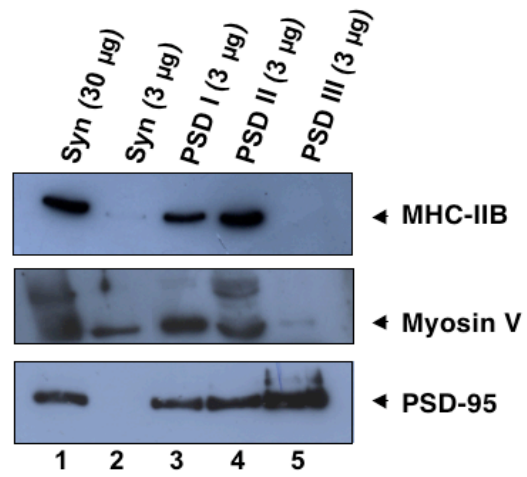
B



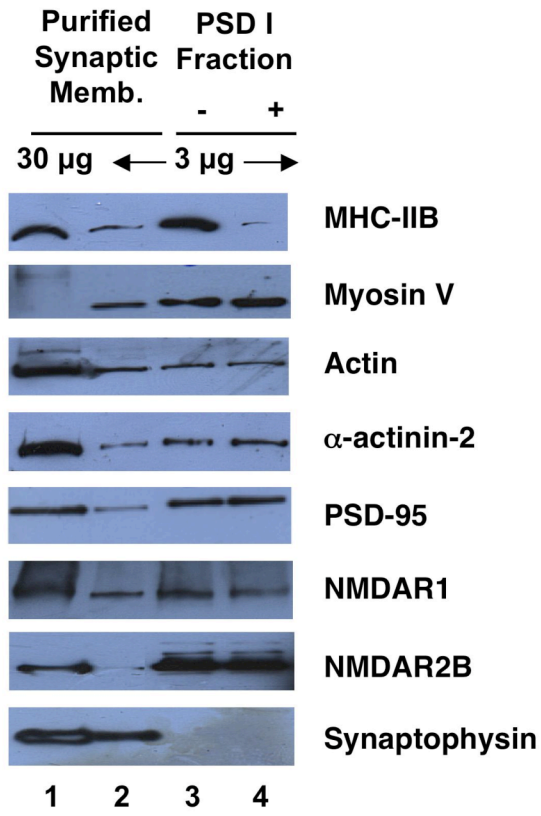
Ishmael et al. Figure 5



Ishmael et al. Figure 6



Ishmael et al. Figure 7



Supplementary Table S1: Proteins identified on the basis of a single peptide

Protein	Accession Number	Category	Peptides	Probability Based Mowse Score
Tenascin-R precursor (Restrictin / Janusin)	Q8BYI9	Cell adhesion	1	99
Neurocan (chondroitin sulfate proteoglycan 3)	P55066	Cell adhesion	1	94
Solute carrier 25 member 4	P48962	Mitochondria	1	56
Neural cell adhesion molecule (N-CAM)	P13595	Cell adhesion	1	44
Sodium/potassium-transporting ATPase alpha-chain	Q8VDN2	Receptors and channels	1	37
Syntaxin-binding protein 1	O08599	Membrane trafficking	1	89
Heat shock cognate 71 kDa protein	P63017	Chaperone	1	83
Excitatory amino acid transporter 2	P43006	Receptors and channels	1	113
Paralemmin (PALM)	Q9Z0P4	Membrane dynamics	1	65
Ciliary neurotrophic factor receptor alpha precursor	O88507	Receptors and channels	1	55
Opioid-binding protein	P32736	Cell adhesion	1	36
Neurotrimin precursor	Q99PJ0	Cell adhesion	1	36
Alpha-centractin	P61164	Cytoskeleton Actin	1	132
Pyruvate dehydrogenase E1 component alpha subunit	P35486	Metabolism	1	122
Integrin-associated protein (IAP)	Q61735	Cell adhesion	1	64
Neuronal growth regulator 1 precursor	Q80Z24	Cell adhesion	1	54
Synaptosomal-associated protein 25A (SNAP)	P36977	Membrane trafficking	1	85

